Online Dosimetry Based on Optically Stimulated Luminescence Materials

J.-R. Vaillé, F. Ravotti, *Student Member, IEEE,*, P. Garcia, M. Glaser, S. Matias, K. Idri, J. Boch, *Member, IEEE*, E. Lorfèvre, P. J. McNulty, F. Saigné, and L. Dusseau, *Senior Member, IEEE*

***Abstract*—A version of the Optically Stimulated Luminescence (OSL) sensor specifically developed to monitor the dose online in radiation facilities is presented and calibrated with ^{60}Co. The lowest dose measurable at the extremity of a 20 m cable is 0.3 mGy.**

***Index Terms*—Online dosimetry, Optically Stimulated Luminescence (OSL), protons.**

I. Introduction

An integrated radiation sensor using Optically Stimulated Luminescence (OSL) was presented in a previously published work [1]–[3]. The device was specially designed to address the concern of the dose measurement aboard spacecrafts. Its main characteristics were: 1) a sensitivity of 10 mGy, 2) a dynamic range of four orders of magnitude, 3) a power consumption close to zero except for the 4 second reading time. During the OSL reading process, the trapped carriers are released which resets the sensor. As a consequence, it is always possible to choose an irradiation/reading cycle that prevents the device from saturating. The above features make the OSL an interesting candidate, not only to measure the dose received orbit by orbit aboard spacecrafts but also to monitor the environment in large radiation facilities, like reactor and accelerators. A preliminary evaluation of the OSL sensor was also conducted at CERN [4] as a part of the RADMON (LHC Experiment Radiation Monitoring) project at the LHC [5]. In the framework of the RADMON program, the feasibility of an online system integrating three types of dosimeters is under investigation. In particular with an integrated system, the long-term Total Ionizing Dose (TID) is monitored with RadFETs [6], [7], forward biased p-i-n diodes provide informations on the cumulative displacement damage effects, and the OSL sensor, reset after each reading, has to contribute to the measurements of the periodical variations of the dose. The first experiments carried out in hadron fields at the CERN Proton Synchrotron accelerator [4] have shown the interest in the OSL sensor, but showed that it had to be modified to take into account the specificity of the LHC environment. Three major concerns were raised. First of all, the OSL was designed as a device to be mounted directly on a PCB. In the case of the LHC, the signals from several sensors are to be conveyed through a 20 m line toward the data acquisition system that remains outside the exposed area as shown in Fig. 1.

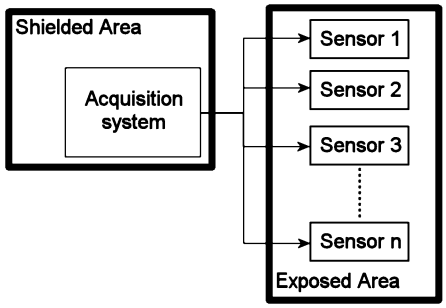

Fig. 1. Multiple OSL sensors dosimetry system example.

During the first irradiation campaign, the electromagnetic environment caused perturbation, and the sensor output stage was hardly able to drive a 5 m cable. The second problem was the sensitivity. It is required that the OSL dosimeter can be used to monitor the dose in highly exposed structures, but also as an ambiance detector in a shielded areas. The current sensitivity of 10 mGy did not meet this last requirement. Finally, the sensor hardened for space conditions would not survive the very harsh environment of the LHC experiments [8]. This paper summarizes the modifications brought to the sensor in order to address the sensitivity, hardness and remote reading problems. In the first section, the principle of the OSL sensor is reviewed. In section two, the new architecture developed for the online sensor is presented. A prototype was assembled and calibrated with a ^{60}Co gamma source in online conditions, including the use of a 20 m cable. The sensor was used to measure the dose deposited by a 110 MeV proton beam at the Centre de Proton Therapy d'Orsay (CPO) during an experiment which aimed at reproducing the dose rates encountered in orbit, and during a periodic flight through the South Atlantic Anomaly (SAA). The results obtained are presented and discussed in the last section.

II. Review of the Sensor

A. Sensor Principle

The OSL sensor is extensively described in [1]–[3], [6], and [10]. Ionizing radiation creates a large amount of electron–hole pairs in the OSL material. A fraction of these carriers are trapped

Manuscript received July 8, 2005; revised August 25, 2005.

J.-R. Vaillé, P. Garcia, J. Boch, F. Saigné, and L. Dusseau are with the CEM2 UMR CNRS 5507, Université Montpellier II, F-34095 Montpellier Cedex 5, France (e-mail: vaille@cem2.univ-montp2.fr).

F. Ravotti and M. Glaser are with the TS and PH Department, CERN, Geneva 23,CH-1211, Switzerland.

S. Matias is with Oncogard, 30100 Ales, France.

K. Idri is with Unité de Physique Centre Val d'Aurelle, 34298 Montpellier, Cedex 5, France.

E. Lorfèvre is with the Centre National d'Etude Spatiale, 31401 Toulouse, Cedex 9, France.

P. J. McNulty is with Clemson University, Clemson, SC 29634 USA.

Digital Object Identifier 10.1109/TNS.2005.860707

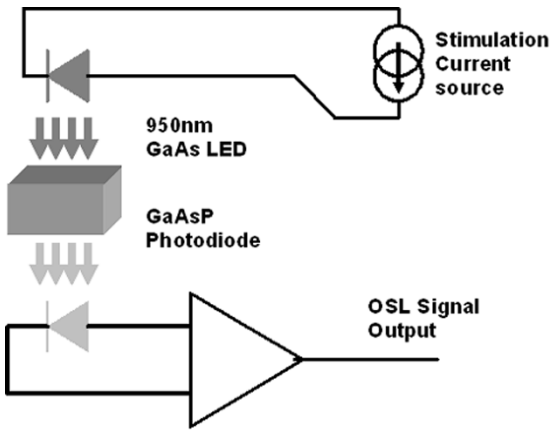

Fig. 2. Principle of the basic OSL sensor.

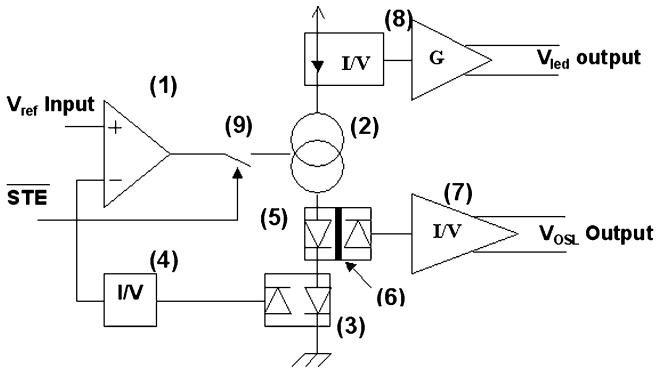

Fig. 3. Principle of the online OSL sensor architecture: (1) opamp; (2) voltage controlled current source; (3) feedback cell (IR Led + Si photodiode); (4) passive current–voltage converter; (5) measure cell (IR LED + GaAsP photodiode); (6) OSL layer (7) active current–voltage converter; (8) LED's current monitoring; and (9) stimulation enable switch.

on energy levels located in the wide band gap of the insulator. Some of this charge will remain trapped for a period of time depending on both the temperature and the activation energy of the traps. Unlike the thermal anneal used for thermo luminescent materials, an optical stimulation will provide the energy necessary to release the charges. A subsequent radiative recombination may be observed. Quantifying the amount of emitted light makes it possible to evaluate the dose. The basic structure of the integrated dosimeter is presented on Fig. 2. A 950 nm infra-red surface mount Light Emitting Diode (LED) provides the stimulation. The luminescence is collected by means of a GaAsP photodiode. The GaAsP wide band gap makes it possible to discriminate the green luminescence from the infra-red stimulation. The 300 μm OSL layer is directly sandwiched between the LED and the photodiode. The power consumption is limited to the bias current in the LED during stimulation that is 45 mA during a few seconds under a 1.5 V bias voltage (cf. Section III). The whole sensor fits in a sugar cube volume and it weights no more than 3 g.

B. New Architecture for Online Dosimetry

The online sensor is based on the structure developed for in flight applications [3]. In the new architecture, the output amplifiers are replaced by two differential outputs. The aim of these modifications is to increase the signal over noise ratio of the output voltage. In the previous paper [3], it has been shown that displacement damage effects decreased the emission of the LED, impacting directly the sensitivity of the sensor. A feedback loop was then introduced to compensate the emission loss by increasing the current in the stimulation LED. This solution solved the problem of the sensitivity loss [3], but in the meantime introduced an unexpected effect: it was observed that spikes occurring during a power-on cycle or due to single event effects could trigger accidentally the reading process, resulting in a loss of information. This problem was fixed by the addition of a validation switch between the differential amplifier and the controlled current source. No current is allowed in the LED, unless the Stimulation Enable (STE) line is validated, hence no more accidental reading. The block diagram of the new structure is presented in Fig. 3.

III. Reading Circuitry

The whole sensor is driven by a simple four twisted pair cable: two wires and the ground for the power supply ($\pm$5 V), two wires for the sensor control (V_{REF} and STE), two wires for both the V_{LED} and V_{OSL} output. In order to improve the signal over noise ratio, the V_{OSL} twisted pair is connected to a limited bandwidth instrumentation amplifier (PGA204 with a voltage gain of 100). The amplifier output and the V_{LED} twisted pair are connected to a National Instrument DAQPad-6020E (Multifunction I/O for USB). Two differential analog input are used to measure both the OSL signal (V_{OSL}) and the V_{LED} voltage (proportional to the stimulation current), One analog output is used to provide the V_{REF} voltage and a digital output to provides STE signal. During a reading request, the STE pin is set to a zero logic level, which enables stimulation. The acquisition starts and after a short delay, an analog level is applied to the V_{REF} p-i-n. During the reading process ($\sim$4 s), the OSL signal is sampled, stored and the peak value extracted, yielding the value of the dose after proper calibration. The readout setup of the sensor is presented in Fig. 4.

IV. Experiments

A. Calibration With ^{60}Co

The results presented in this paper derive from the calibration curves recorded with the ^{60}Co gamma source available at the Centre d'Electronique et de Micro-Optoelectronique de Montpellier. Measurements have been made with a 20 m cable in order to demonstrate the sensor remote capability. In all the experiments described, V_{REF} is set to 1.5 V, corresponding to a 45 mA stimulation current in the LED. In operational conditions, the feedback loop can increase the forward current in the LED up to 100 mA, which is enough to compensate a severe radiation-induced degradation. The ^{60}Co irradiation was performed with several dose rates and the incremental doses where obtained by increasing the irradiation time. The curves in Fig. 5 present the mean value of three OSL signal measurements recorded at the output of the instrumentation amplifier. The signal versus dose response exhibits a good linearity over the four orders of magnitude investigated.

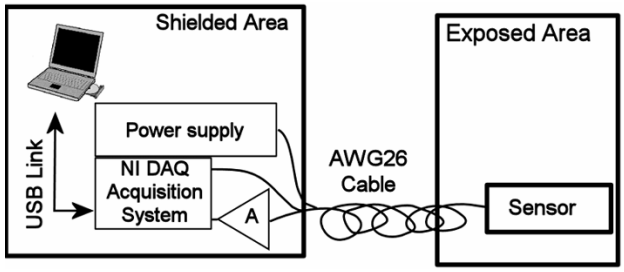

Fig. 4. Readout principle of the dosimeter.

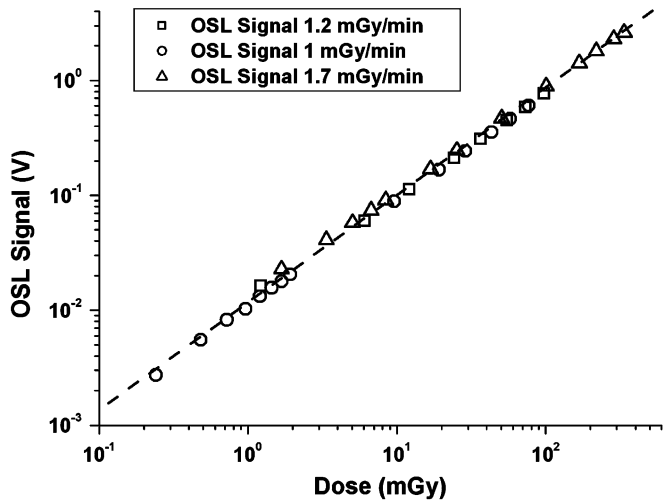

Fig. 5. Calibration curve of an OSL dosimeter irradiated with ^{60}Co gamma rays at the extremity of a 20 m cable for different dose rate.

The online automated data acquisition setup makes possible to repeat the experiments without moving the sensor and obtain statistics on the signal. The mean value and the standard deviation were calculated on a sample of 20 measurements taken in the same conditions without moving the sensor and this, for different dose.

The repeatability of the measurement as a function of dose can be estimated by defining the ratio

$$R = \frac{\sigma}{\overline{\mathrm{OSL}}} \times 100 \tag{1}$$

where σ is the standard deviation and $\overline{\mathrm{OSL}}$ is the average value of the 20-measurement set. So, an decreasing value of R means an better repeatability. Table I summarizes the obtained results.

As shown on Table I, the standard deviation remains almost constant. The variations of R versus dose have been plotted on Fig. 6. This curve was obtained for a worst case value of the standard deviation of 3.5×10^{-4}. The ratio R is above 10% for doses below 0.3 mGy but drops rapidly below 5% for a dose of 0.8 mGy.

B. Efficiency of the Dosimeter Hardening Solution

The hardening solution developed for the sensor is presented in [3]. It consists in a feedback loop that ensures a constant optical stimulation of the OSL material. In order to verify the behavior of this new architecture under irradiation, the dosimeter was exposed to a 17 MeV electron beam and a fluence of 1.3×10^{12} cm^{-2}, following the test protocol described below, and performed at the Centre de Lutte Contre le Cancer Val d'Aurelle, in Montpellier, with a Saturn 20 linear accelerator.

TABLE I
SUMMARY OF THE SENSOR REPEATABILITY

Dose (mGy)	Average OSL signal (V)	Standard deviation (V)	R (%)
0.24	2.7×10^{-3}	2.6×10^{-4}	9.6
0.48	5.5×10^{-3}	3×10^{-4}	5.4
1.2	1.3×10^{-2}	3.2×10^{-4}	2.5
19.2	1.7×10^{-1}	3×10^{-4}	0.2

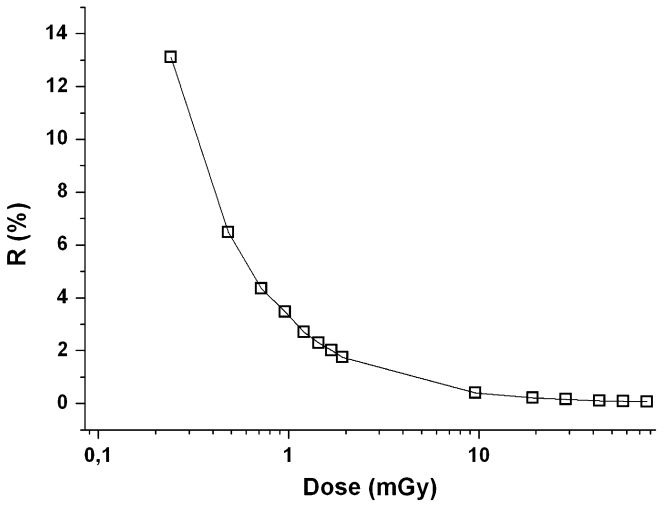

Fig. 6. Evolution of the ratio between the standard deviation and the mean value as a function of dose.

During the first step of the protocol, the preirradiation output signal sensor is measured for a low reference total ionizing dose deposited with a 18 MV RX beam. The second step, an irradiation performed with a 17 MeV electron beam (9.3×10^{10} e$^-$·cm^{-2} (about 50 Gy)) aims at degrading the constituting devices of the sensor (the used dose in this step is about 1000 times higher than the doses used to calibrate the sensor). During the third step, the response of the dosimeter is measured in the same conditions used in step #1. The flow chart of this method is presented in the Fig. 7. If the feedback look compensates the degradation of the LED, then the response should remain constant.

The results obtained are presented on the Fig. 8 that plots the average normalized value of the OSL signal recorded for three measurements performed in the condition described above, before and after each step of 17 MeV electron irradiation.

This curve shows that the dispersion in the results remains lower than 10%. Moreover, the values recorded fluctuate around an average value and no decreasing trend is observed. Those fluctuations remain within the uncertainty on the fluence delivered by the accelerator. Hence, we can conclude that there is no significant degradation for an electron fluence up to 1.3×10^{12} cm^{-2} ($\sim 8 \times 10^{10}$cm^{-2} 1 MeV equivalent)

C. Monitoring of a 110 MeV Proton Beam

The application presented in this section is a joint experiment between the University of Montpellier and Centre National

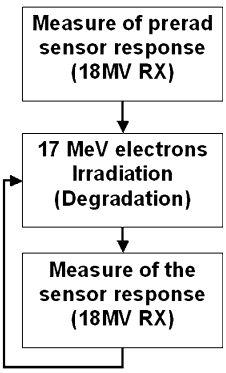

Fig. 7. Flow chart of the test method used to characterize the radiation hardness of the sensor.

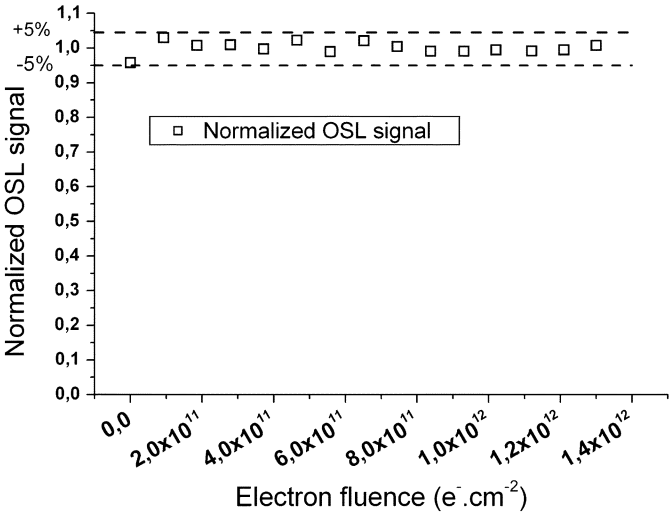

Fig. 8. Evolution of the sensor normalized output voltage for a small reference dose versus the 17 MeV electron fluence.

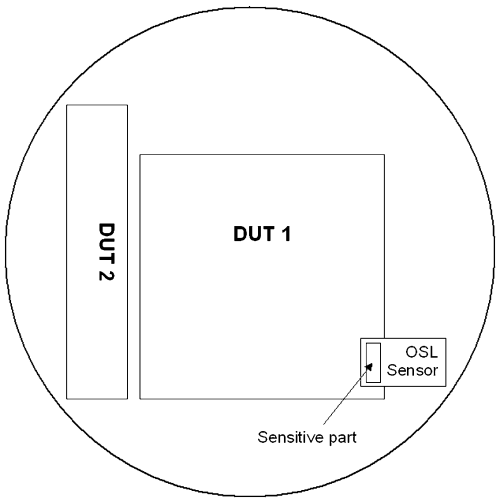

Fig. 9. Mechanical diagram of the proton irradiation experimental setup. The proton beam diameter is 130 mm.

d'Etudes Spatiales (CNES). For CNES, the primary goal of the experiment was to irradiate photonic devices in conditions that would model as closely as possible the environment encountered during a periodical flight into the SAA. The total duration of the irradiation is 12 hours with an average dose rate of 10 rad·h^{-1} (100 mGy·h^{-1}).

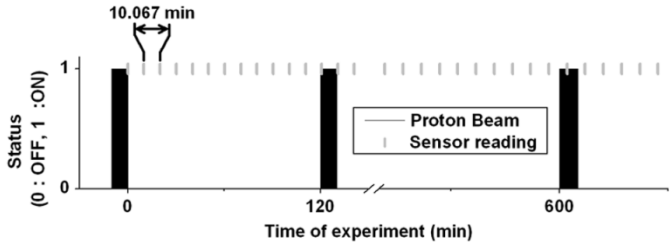

Fig. 10. Chronogram of the proton irradiation experiment.

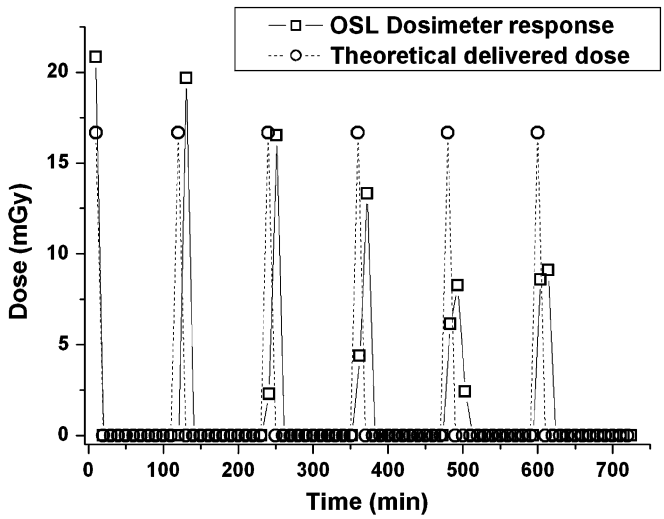

Fig. 11. Dose measured by the sensor compared to theoretical dose. The measured dose for each batch is obtained by summing the two or three next measures.

The periodical flight through the SAA is modeled by a pulsed 110 MeV proton beam, switched ON during 10 min with a period of 120 min. These are marginal conditions for the Medical Cyclotron: the dose rate is much lower than the dose rates used in radiotherapy (Gy·min^{-1}), far below the limit of detection of the standard sensors. As a consequence, CPO could only provide an indication on the dose rate with an uncertainty of 200% on the total dose delivered. In agreement with CNES, it was decided to use the OSL to monitor the dose delivered during the 12 hours of the experiment. The experimental setup is presented in Fig. 9.

The planning of the experiment is presented on Fig. 10. The first measurement is taken at the end of the first proton run and repeated with a period of 10 min. The timing of the beam runs, more difficult to control, did not follow exactly the 10 min period, which resulted in a shift in the measurement steps, and more than one measurement per run. The dose recorded as a function of time is plotted in Fig. 11. It is then possible to evaluate the dose delivered to the Device Under Test (DUT) during each run of irradiation, by summing the results of the measurement made during each run. The results, presented in Fig. 12 are consistent with the levels of dose expected. Let's note that the uncertainty on the fluence delivered was initially 200%.

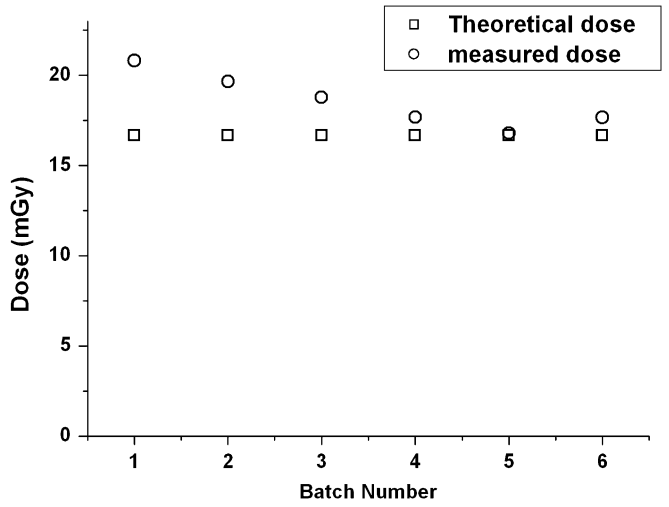

Fig. 12. Integral measured dose compared to the theoretical integral dose for each batch of the proton beam.

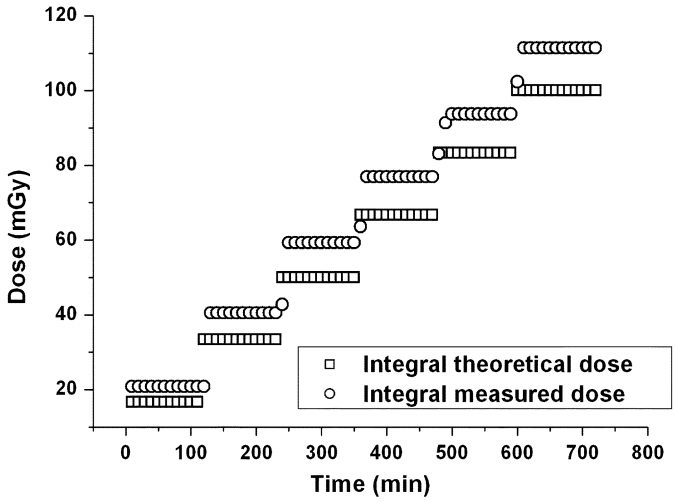

Fig. 13. Integral measured dose and theoretical integral dose versus experiment time.

Fig. 13 presents the Total Ionizing Dose delivered as a function of time. The results of the OSL measurement are compared with an extrapolation of the calibration curve recorded by the standard sensors used in radiotherapy. It is understood that those sensors are unable to provide any information in the range of dose investigated in this paper. It appears that the dose delivered, 111 mGy, is slightly higher than the value expected, but the order of magnitude is respected.

V. Conclusion

A new version of the OSL integrated sensor was developed to match the requirements of an online dose monitoring in large radiation facilities such as LHC. The problems of sensitivity, radiation hardness and remote sensing have been successfully addressed. The experiment presented in this paper aimed at reproducing conditions similar to those encountered on a satellite. The dose delivered was sampled during, 12 hours with an OSL sensor working in an autonomous mode. The electromagnetic environment surrounding the cyclotron did not cause any perturbation. This result is especially encouraging for future applications, such as the DIME experiment to be flown on the NASA Space Environment Testbed (SET1) [12] satellite and Influence of Space Radiation on Advanced Components New Generation (ICARE NG) from CNES.

Acknowledgment

The authors would like to thank the Centre National d'Etudes Spatiales for its long-term support on the OSL project.

References

[1] L. Dusseau, D. Plattard, J. R. Vaillé, G. Polge, G. Ranchoux, F. Saigné, J. Fesquet, R. Ecoffet, and J. Gasiot, "An integrated sensor using optically stimulated luminescence for in flight dosimetry," *IEEE Trans. Nucl. Sci.*, vol. 47, no. 6, pp. 2412–2416, Dec. 2000.

[2] D. Plattard, G. Ranchoux, L. Dusseau, G. Polge, J.-R. Vaille, J. Gasiot, J. Fesquet, R. Ecoffet, and N. Iborra-Brassart, "Characterization of an integrated sensor using optically stimulate luminescence for in-flight dosimetry," *IEEE Trans. Nucl. Sci.*, vol. 49, no. 6, pp. 1322–1326, Dec. 2002.

[3] J.-R. Vaille, S. Ducret, K. Idri, F. Saigne, S. Matias, N. Iborra, R. Germanicus, R. Ecoffet, and L. Dusseau, "Hardening of a radiation sensor based on optically stimulated luminescence," *IEEE Trans. Nucl. Sci.*, vol. 50, no. 3, pp. 2358–2362, Dec. 2003.

[4] F. Ravotti, M. Glaser, M. Moll, K. Idri, J.-R. Vaille, H. Prevost, and L. Dusseau, "Conception of an integrated sensor for the radiation monitoring of the CMS experiment at the large hadron collider," *IEEE Trans. Nucl. Sci.*, vol. 51, no. 6, pp. 3642–3648, Dec. 2004.

[5] F. Ravotti, M. Glaser, K. Idri, J.-R. Vaillé, H. Prevost, and L. Dusseau, "Optically stimulated luminescence materials for wide-spectru neutron measurement at CERN," in *Proc. RADECS 2004*, 2004, pp. 299–304.

[6] B. O'Connell, C. Conneely, C. Mc. Carthy, J. Doyle, W. Lane, and L. Adams, "Electrical performances and radiation sensitivity of stacked PMOS dosimeters under bulkbias control," *IEEE Trans. Nucl. Sci.*, vol. 45, no. 6, pp. 2689–2694, Dec. 1998.

[7] A. G. Holmes-Siedle and L. Adams, "RadFETs: A review of the use of metal–oxide–silicon device as integrating dosimeters," *Rad. Phys. Chem.*, vol. 28, no. 2, pp. 235–244, 1986.

[8] M. Huhtinen, "Radiation environment simulations for the CMS detector," CERN, Geneva, Switzerland, CMS Tech. Note 95-198, 1995.

[9] L. Dusseau, G. Ranchoux, G. Polge, D. Plattard, Y. Magnac, F. Saigné, J. C. Bessière, J. Fesquet, and J. Gasiot, "High energy electron dose-mapping using optically stimulated phosphors," *IEEE Trans. Nucl. Sci.*, vol. 46, no. 6, pp. 1757–1761, Dec. 1999.

[10] K. Idri, L. Santoro, E. Charpiot, J. Herault, A. Costa, N. Ailleres, R. Delard, J.-R. Vaille, J. Fesquet, and L. Dusseau, "Quality control of intensity modulated radiation therapy with optically stimulated luminescent films," *IEEE Trans. Nucl. Sci.*, vol. 51, no. 6, pp. 3638–3641, Dec. 2004.

[11] L. Dusseau, G. Polge, L. Albert, Y. Magnac, J. C. Bessière, J. Fesquet, and J. Gasiot, "Irradiated integrated circuits dose-attenuated mapping using optically stimulated phosphors for packaging dosimetry," *IEEE Trans. Nucl. Sci.*, vol. 45, pp. 2695–2699, 1998.

[12] B. Sherman and M. Cuviello, "NASA's LWS/SET technology experiment carrier," in *Proc. IEEE Aerospace Conf. 2003*, vol. 1, Mar. 8–15, 2003, pp. 1–435.